The Linnean Society of London ZOOLOGICAL Journal of the Linnean Society

Zoological Journal of the Linnean Society, 2012, **164**, 18–35. With 9 figures

An integrative approach to characterize cryptic species in the *Thoracostoma trachygaster* Hope, 1967 complex (Nematoda: Leptosomatidae)

DANIEL APOLÔNIO SILVA DE OLIVEIRA[1], WILFRIDA DECRAEMER[1,2], OLEKSANDER HOLOVACHOV[3], JAY BURR[3], IRMA TANDINGAN DE LEY[3], PAUL DE LEY[3], TOM MOENS[4] and SOFIE DERYCKE[4]*

[1]*Department of Biology, Ghent University, Ghent, K.L. Ledeganckstraat 35, 9000 Ghent, Belgium*
[2]*Royal Belgian Institute of Natural Sciences, Vautierstraat 29, 1000 Brussels, Belgium*
[3]*Department of Nematology, University of California, Riverside, 900 University Drive, Riverside, CA 92521, USA*
[4]*Department of Biology, Marine Biology section, Ghent University, Krijgslaan 281, S8, 9000 Gent, Belgium*

Received 28 December 2010; revised 6 May 2011; accepted for publication 9 May 2011

Nematode diversity may seriously be underestimated when taking into account cryptic speciation. *Thoracostoma trachygaster* is commonly found in kelp holdfasts along the California coastline and was recently shown to consist of at least two distinct molecular clades (I and II). Here, we provide detailed morphological analysis of both clades, based on measurements taken from video vouchers of respectively eight and 16 individuals from the previous study, as well as 80 newly collected specimens from four Californian beaches. The latter were vouchered, measured, and then subjected to molecular analyses of the mitochondrial cytochrome oxidase c subunit I (COI) gene, and the ribosomal D2D3 and internal transcribed spacer (ITS) regions. This integrative approach shows that the three molecular clades are phylogenetically and morphologically distinct species, but a combination of morphological characters is needed to distinguish them. Two new species, ***Thoracostoma fatimae* sp. nov.** and ***Thoracostoma igniferum* sp. nov.**, are identified and described. The spicule length of *T. fatimae* sp. nov. is significantly shorter than that of *T. trachygaster*. *Thoracostoma igniferum* sp. nov. can be distinguished by the irregular posterior edge of the cephalic capsule and the two internal subdorsal tropis-like projections in the wall of the cephalic capsule, which are lacking in *T. fatimae* sp. nov. and *T. trachygaster*.

doi: 10.1111/j.1096-3642.2011.00758.x

ADDITIONAL KEYWORDS: California – COI – D2D3 – integrative taxonomy – ITS – marine – morphology.

INTRODUCTION

The presence of cryptic diversity across the tree of life has been recognized for a long time (Bickford *et al*., 2007), and has strong implications for conservation and ecosystem functioning (Bickford *et al*., 2007; Harmon *et al*., 2009). This cryptic diversity may be more common in marine environments because here, chemical cues are more important for mate recognition than morphology (Knowlton, 2000; Goetze & Kiørboe, 2008). One group of organisms that is particularly abundant in marine environments is nematodes (Lambshead, 2001; Floyd *et al*., 2002). Although only about 27 000 species have been formally described (Hugot, Baujard & Morand, 2001; Coomans, 2002), total extant species diversity estimates are likely to be several orders of magnitude higher (Lambshead, 2001). Nematodes have a well-developed chemosensory system (O'Halloran, Fitzpatrick &

*Corresponding author. E-mail: s.derycke@UGent.be

Burnell, 2006) and may attract the opposite sex by pheromones (Edison, 2009). Describing and identifying nematode species is often challenging, because related species may show high phenotypic plasticity (Coomans, 2002; Nadler, 2002; Powers, 2004) and few to no easily observable diagnostic morphological characters (e.g. Tandingan De Ley *et al*., 2007). Consequently, cryptic diversity within marine nematodes may be substantial (Derycke *et al*., 2005, 2007a, 2010a).

Cryptic species are often discovered by sequencing multiple independently evolving gene regions and looking for phylogenetic congruence amongst them (Adams, 2001). However, DNA sequence analyses are not free of inconsistencies or subjectivity in their own right: saturation effects or incongruence of phylogenetic signal in different data sets may obscure species boundaries (Dolphin *et al*., 2000; Sanderson & Shaffer, 2002). Therefore congruence between molecular and morphological data may help overcome the limitations of either data set for the purposes of species boundary delimitation (Wiens & Penkrot, 2002).

Few integrative studies have been conducted to date on nematodes (e.g. De Ley *et al*., 1999; Gozel *et al*., 2006; Holovachov *et al*., 2009) and even fewer on free-living marine nematodes (e.g. De Ley *et al*., 2005; Fonseca, Derycke & Moens, 2008; Neres *et al*., 2010; Pereira *et al*., 2010). This is in part a consequence of the destructive nature of molecular analyses for small-sized organisms: because the entire organism is required for DNA extraction, special vouchering methods are needed prior to molecular analysis to preserve an unambiguous link between the DNA sequences and the morphology of each specimen (De Ley & Bert, 2002; Abebe *et al*., 2004; De Ley *et al*., 2005; Derycke *et al*., 2010a). Moreover, the potential of species to exhibit substantial phenotypic plasticity (Kiontke & Fitch, 2010), as well as intricate patterns of co-occurrence (Suatoni *et al*., 2006; Derycke *et al*., 2007a, 2008b; Nygren, Eklöf & Pleijel, 2010), implies that a large number of specimens from several populations are required to screen genetic and morphological variability accurately (Nadler, 2002). Such an approach can highlight subtle morphological differences between genetically distinct marine nematode species (e.g. *Pellioditis marina* and *Halomonhystera disjuncta*, Fonseca *et al*., 2008; Derycke *et al*., 2008a).

Along the coast of California, two leptosomatid species (*Thoracostoma trachygaster* Hope, 1967 and *Thoracostoma microlobatum* Allgén, 1947) are frequently found in association with holdfasts such as *Egregia* sp. and *Macrocystis* sp. (Hope, 1967) as well as other common algal and epigrowth communities (Holovachov O & De Ley P, unpubl. data). A population genetic study on *T. trachygaster* revealed genetic structuring along the Californian coastline, with indications of genetic breaks around Point Conception and the Los Angeles region (Derycke *et al*., 2010a). Moreover, two distinct molecular clades were found occurring sympatrically in locations along the California coastline.

Here, we investigated whether the molecular lineages observed in *T. trachygaster* are also morphologically distinct. The genus *Thoracostoma* can be recognized by the presence of a well-developed cephalic capsule with ventral tropis in all known species (Wieser, 1956; Mawson, 1958). The number and shape of perforations in the cephalic capsule have been used to distinguish species despite high levels of intraspecific variation (Filipjev, 1916). The spicules, precloacal papillae and supplements, and secondary sexual features (a single median ventral supplement and a series of subventral precloacal and postcloacal setae) may also be important for species differentiation.

The goals of this work were to investigate whether the highly divergent molecular lineages found in Derycke *et al*. (2010a) are morphologically and/or morphometrically distinct and if so, to provide species descriptions of the new *Thoracostoma* species.

MATERIAL AND METHODS

MORPHOLOGY OF *THORACOSTOMA TRACHYGASTER* HOPE, 1967

The genus *Thoracostoma* can be distinguished from the related genera *Pseudocella* and *Deontostoma* because of the presence of eyespots and a tropis. The tropis is absent in *Deontostoma*, and can be either absent or present in *Pseudocella*. The latter genus lacks eyespots (Hope, 1967).

Thoracostoma trachygaster is a large nematode (5–9.8 mm long) with a blunt tail and anterior end. It differs from all other *Thoracostoma* species by the presence of the scabrous gaster in males and the presence of cuticular granules surrounding the vulva in females (Hope, 1967). There is a well-developed sclerotized cephalic capsule, a shield-shaped amphidial fovea, and two distinct eyespots with pigment cup and refractile body located anteriorly in the neck region. The anterior sensilla are arranged in a 6 + 10 pattern and are 2–4 μm long. Cervical setae are organized in six distinct series between the eyespots and the cephalic suture, in four series (two subdorsal and subventral) after the eyespot, and randomly after the nerve ring. The cephalic capsule is without distinct anterior lobes, except for the ventral tropis extending to the anterior end of the head, and with six posterior lobes separated by incisions. Males are diorchic with opposed

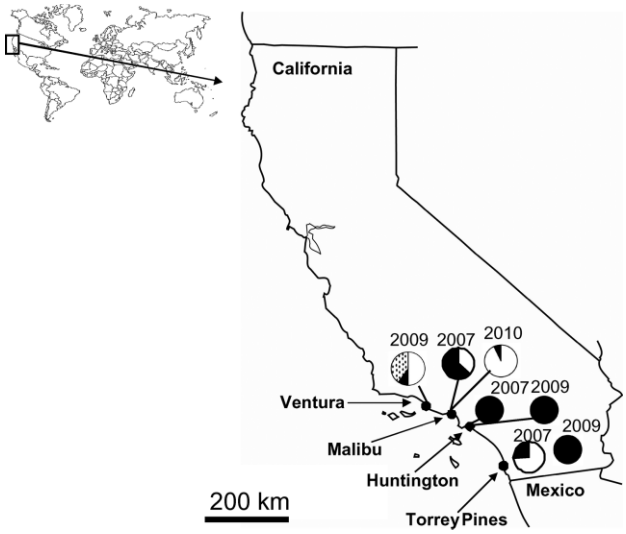

Figure 1. Sampling points along the California coastline in 2007, 2009, and 2010. White, black, and the dotted area represent clades I, II, and III, respectively.

testes. The spicules are 104–169 μm long and wider in the middle region. The gubernaculum is duplicated and at the proximal end there is a membrane surrounding the spicule. There is a ventromedian cyathiform winged supplement. The females are amphidelphic with reflexed ovaries. There are intracuticular granules surrounding the transverse vagina. *Thoracostoma trachygaster* resembles the congeneric and sometimes co-occurring species *Thoracostoma microlobatum* but the adults can be distinguished from the latter by the absence of perforations in the head capsule, the presence of intracuticular granules surrounding the vulva, and the shorter body length (maximum of 8.9 mm in *T. trachygaster* vs. 11.3–19.5 mm in *T. microlobatum*).

Nematode isolation and vouchering

In 2007 nematodes were collected at nine different localities from a variety of *Macrocystis* holdfasts that had been washed ashore on beaches along the California coastline (Derycke *et al*., 2010a). All specimens were video vouchered. Males and females from several populations from both clades were selected to study their morphology in detail. In addition, new specimens were collected in 2009 and 2010 from the two beaches where both clades co-occurred in 2007 (Torrey Pines and Malibu beach), as well as from a location where only clade II was found in 2007 (Huntington Beach) and from a new locality north of Malibu Beach (Ventura beach) (Fig. 1, Table 1). In the laboratory, extraction and isolation were carried out according to Derycke *et al*. (2010a). Nematodes were mounted on temporary slides with sterile distilled water and were observed at different magnifications using a light microscope (Leica DAS Mikroskop type R) with differential interference illumination, and equipped with a Leica DFC420 camera. The entire habitus and selected body regions with important taxonomic structures (head, mid-body, and tail region) were photographed and measured *in silico* using Leica Application Suite v. 3.4.1.

Table 1. Sampling locations along with their coordinates and the number of specimens (*N*) belonging to the *Thoracostoma trachygaster* species complex collected in 2009 and 2010

Location names	Beach coordinates	2009 *N*	2010 *N*
Ventura	34°16′30″N 119°13′40″W	30	–
Malibu	34°1′50″N 118°46′43″W	–	13
Huntington	33°41′34″N 118°0′1″W	6	–
Torrey Pines	32°53′23″N 117°14′54″W	31	–

'–', no holdfasts were collected.

Molecular analyses

After the vouchering procedure, specimens were immediately cut into four pieces: head and tail (males) or vulva (females) regions were stored in DESS (Yoder *et al.*, 2006) in 0.5 mL centrifuge tubes for morphological analysis. The remaining two body parts were stored in separate centrifuge tubes with 25 μL Worm Lysis Buffer (50 mM KCl, 10 mM Tris–HCl pH 8.3, 2.5 mM $MgCl_2$, 0.45% nonyl phenoxypolyethoxylethanol (NP40), 0.45% Tween 20) and stored at –20 °C until DNA extraction. The samples were digested for 1 h at 65 °C and for 10 min at 95 °C with 2 μL of Proteinase K (10 mg mL^{-1}). Tubes were centrifuged at maximum speed (21 000 *g*) for 1 min and stored at –20 °C. All specimens were subjected to PCR to amplify a 396 bp fragment of the cytochrome oxidase c subunit I (COI) gene with the primers JB3 and JB5 (Derycke *et al*., 2005). PCR was performed in 25 μL reaction mixtures and contained: 0.125 μL TOPTAQ polymerase (Qiagen), 2.5 μL of 10 × PCR buffer with 15 mM $MgCl_2$, 2.5 μL coral load PCR buffer 10 ×, 2 μL $MgCl_2$ 25 mM, 0.5 μL deoxynucleotide triphosphate (10 mM), 1 μL of each primer (25 μM), and 1 μL DNA diluted tenfold. For COI, the thermocycling conditions were: 94 °C for 5 min; 35 cycles of 94 °C for 30 s, 50 °C for 30 s and 72 °C for 30 s, plus a final extension step at 72 °C for 10 min.

To confirm the clades obtained in the COI tree, two nuclear regions were amplified for six randomly selected specimens from a newly discovered clade (clade III). The D2D3 region of the large subunit of the nuclear ribosomal DNA was amplified with the primers D2A and D3B whereas the internal transcribed spacer (ITS) region was amplified using the primers Vrain2F and Vrain2R with thermocycling conditions of Derycke *et al*. (2010a).

The sequencing reaction was performed with the BigDye Terminator v. 3.1 Mix (PE Applied Biosystems) under the following conditions: an initial denaturation of 2 min at 98 °C was followed by 40 cycles of denaturation at 98 °C for 10 s, annealing at 50 °C for 5 s, and extension at 60 °C for 60 s. As we only wanted to verify to which clade the freshly collected specimens belonged, COI was unidirectionally sequenced using the reverse primer JB5. All sequences were cut until they reached the length of the shortest sequence (315 bp). The six specimens from the newly discovered clade were bidirectionally sequenced to obtain and confirm the new COI sequences. For D2D3, both strands were sequenced using the amplification primers. For ITS, the primers Ferris 2F (RGY AAA AGT CGT AAC AAG GT) and VRAIN 2R were used. The Ferris 2F primer is located at the 3′ end of the ribosomal small subunit gene downstream of the VRAIN 2F primer, but is still external to the ITS region. All sequences can be found under GenBank accession numbers FR853134–FR853144.

Data analysis

Phylogenetic analyses

Sequence chromatograms from the three genes (COI, D2D3, and ITS) were analysed with LASERGENE v. 7.1.0 and aligned separately using SEAVIEW v. 4.2 (Galtier, Gouy & Gautier, 1996). Neighbour-joining trees were generated in PAUP* v. 4.0b10 (Swofford, 1998) with bootstrap analyses at 1000 replications. The maximum and minimum pairwise distances within and between COI clades were calculated using the P-distance model in MEGA v. 4.0. (Tamura *et al*., 2007).

Morphometry and morphology

As significant differences were observed between the different vouchering methods (videos versus temporary slides), even after applying a conversion factor between the two systems, the morphometric analysis was divided into two parts. The first part contained 24 adult specimens sampled in 2007 from Malibu Beach, Torrey Pines, and Huntington Beach from clades I (five males, 11 females) and II (seven males, one female). These 24 specimens were measured *a posteriori* from the recorded video images. Selected frames of each video clip were printed on A4 paper with the corresponding scale bar as reference point. According to the image quality and field of view, 13 characters could be reliably measured. The second part consisted of 80 newly collected adult specimens from 2009–2010, which were measured directly from a temporary slide using light microscopy prior to molecular analysis. Here, 20 characters were measured in 52 individuals but 28 individuals permitted fewer than 20 characters to be measured. The 52 individuals with complete biometrics were selected for morphometric analysis. All morphometric data are presented in Tables 3–6.

All morphometric data analyses were performed with the software PRIMER v. 6.1.6 (Clarke & Gorley, 2006). First, multivariate analyses were performed to check if measurements were different when using the video-vouchered specimens from 2007 or the photo-vouchered specimens from 2009–2010. To this end, the 13 characters common to both groups were compared. The data set was standardized and a dissimilarity matrix based on Euclidean distance was constructed. No transformations were carried out. Nonmetric multidimensional scaling (MDS) and one-way Analysis of Similarity (ANOSIM) were performed. Next, the two measuring methods were analysed separately to investigate whether the molecular clades revealed morphological differences. In addition to MDS and one-way ANOSIM, a similarity of percentages (SIMPER) was performed to detect which characters contributed most to the observed differences between clades. For this analysis all characters were used except the sexual ones. Finally, a third analysis was performed using only males (female sexual characters were not significantly different amongst clades) and including sexual characters. Subsequently, a one-way ANOVA was performed on the spicule length, because this character was non-overlapping between clades, using the software STATISTICA v. 7 (StatSoft, Inc., 2004). All assumptions were met. Correlation between morphometric characters was investigated using STATISTICA v. 7. None of the characters had a correlation higher than 0.95. Therefore, the observed groupings were not the result of an artificial clustering.

3D reconstruction

The cephalic capsule is an important structure to differentiate species within the genus *Thoracostoma* (Hope, 1967). Three individuals of each clade (nine individuals) were randomly selected. Nine head sections were mounted in a glycerol-gelatine mixture (60 g distilled water, 10 g gelatine, 70 g glycerol, and 1.4 g phenol) and observed under a light microscope. One slide from clade II and one from clade III were selected for the 3D reconstruction. As the cephalic

capsule from clade I was very similar to that of clade II, it was not included in this analysis. Seventy-three pictures from the two cephalic capsules were taken at different depths. The pictures were used for constructing the 3D model in the software AMIRA 3.1.1. (TGS Software, San Diego, California, USA).

RESULTS

Phylogenetic analysis

A total of 80 new specimens of *T. trachygaster* was collected from the 2009 and 2010 sampling sites and sequenced for the COI gene. Preliminary analyses indicated that two sequences were from individuals of the genus *Pseudocella* Filipjev, 1927 and were therefore designated as outgroups in the most rigorous analysis. The two clades (I and II) found in 2007 were again recovered in the new sample from Malibu and from the new locality Ventura with a bootstrap support of 97 (Fig. 2). Most interestingly, 12 specimens from Ventura formed a well-defined third single sequence branch (clade III) within the nominal species *T. trachygaster*. The COI sequences yielded 19 haplotypes, ten of which were new compared to Derycke *et al*. (2010a). From the newly sequenced specimens, six haplotypes belonged to clade I, 12 to clade II, and only one represented the new clade III (Fig. 2). P-distances for COI within clades ranged from 0–3.7% and between clades from 5.7–13.3% (Table 2). P-distances between the three clades and the congener *T. microlobatum* ranged between 23.9–24.9%.

To investigate this new clade III in more detail, bidirectional COI (396 bp, 237 variable sites, 217 parsimony informative characters), D2D3 (714 bp; 210 variable sites, 136 parsimony informative characters), and ITS regions (1149 bp, 324 variable sites, 315 parsimony informative characters) were sequenced from six randomly chosen clade III specimens. The resulting concatenated alignments (1913 characters, 407 variable sites, 396 parsimony informative sites) yielded a neighbour-joining tree, which also showed the well-supported clade III (Fig. 3). No genetic polymorphism within clade III was observed for either nuclear marker. P-distances between clades I and III ranged between 6.7–6.9% for ITS and between 0.8–1.0% for D2D3. P-distances between clades II and III ranged between 5.2–5.5% for ITS and between 1.0–1.1% for D2D3.

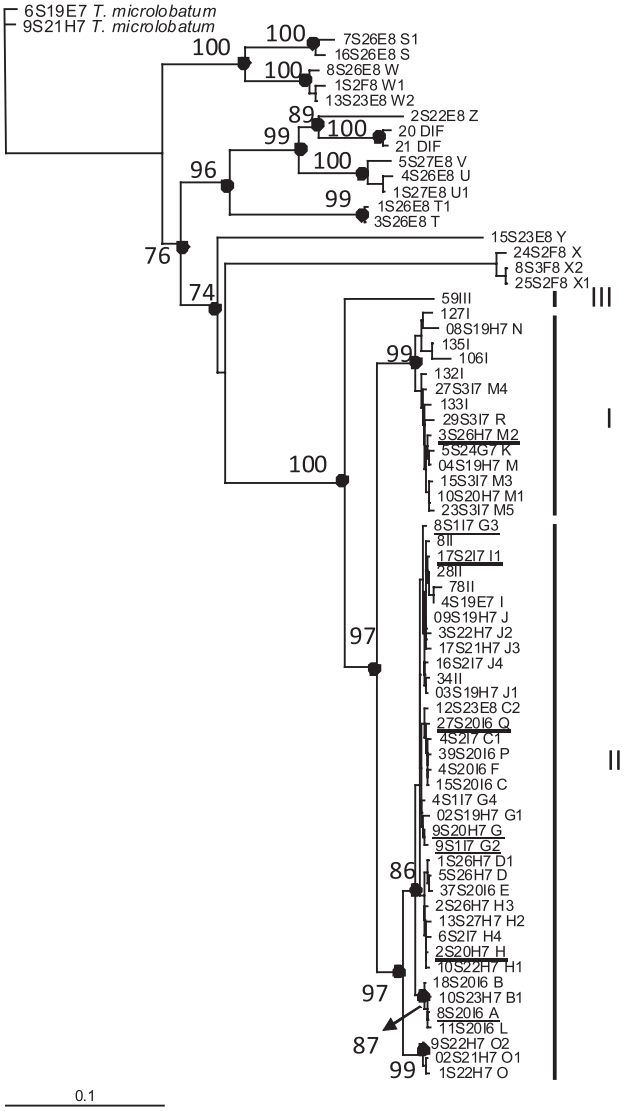

Figure 2. Cytochrome oxidase c subunit I. Neighbour-joining tree based on P-distances with haplotypes from 2007 and the new haplotypes found in 2009 and 2010 (represented by numbers followed by clade – I, II, or III). The haplotypes from clade I and II that were recovered from 2007 appear underlined in the tree. The corresponding taxon names of the other clades can be found in Derycke *et al*. (2010a).

Morphometry

Comparisons between video-recorded and slide-mounted specimens

The MDS based on the 13 morphological characters did not show a clear separation between videos and direct measurements on slides. However, the ANOSIM analysis did show a significant difference ($R = 0.223$, $P = 0.01$). Thus, the two data sets from different methods could not be combined. The SIMPER analysis showed that there was not a strong contribution of any particular character to this difference (individual character contributions lower than 14%), but video measurements systematically yielded lower values than direct measurements on slides.

Table 2. Minimum and maximum cytochrome oxidase c subunit I P-distances within (diagonal) and between clades I, II, and III of the *Thoracostoma trachygaster* species complex

	I	II	III
I	0–0.029		
II	0.057–0.082	0–0.037	
III	0.090–0.109	0.109–0.133	0–0.003

Based on 24 video-vouchered specimens (males and females) from 2007 using the same 13 morphological characters, the two clades (I and II) could be distinguished morphometrically (Fig. 4A, ANOSIM, $R = 0.921$, $P = 0.01$). The SIMPER analysis showed that cephalic capsule length, tail length and body length contributed most to the differentiation of clades I and II (cumulative contribution of 38%).

Based on 20 characters (Tables 3, 4) from the 52 new specimens directly measured from slides, the three clades were separated (Fig. 4B, ANOSIM, $R = 0.36$, $P = 0.01$) and SIMPER showed that body diameter at the base of the pharynx, anal body diameter, and cephalic capsule length were the most important characters to separate clades I and II (cumulative contribution of 27%); body diameter at the base of the pharynx, maximum body diameter, and cephalic capsule width at the posterior edge contributed most to the differentiation of clades I and III (cumulative contribution of 40%); and body length, tail length, and anal body diameter contributed most to the separation of clades II and III (cumulative distribution of 33%). Sexual characters also contributed to the separation of the three clades (ANOSIM $R = 0.528$, $P = 0.001$). Gubernaculum length contributed most to this separation (SIMPER clades I vs. II 15%, I vs. III 17%, II vs. III 20.33%), but nevertheless overlapped between clades. By contrast, the one-way ANOVA showed that spicule length was significantly different between clades I and II ($P < 0.05$) without overlap [average spicule length of 116 µm (100–123 µm) vs. 154 µm (124–173 µm), respectively]. Clade I is generally smaller than clade II [body length average 5.4 mm (4.7–6.0 mm) vs. 6.4 mm (range 4.6–9.8 mm), respectively], but this feature shows high intraspecific variation and is therefore not diagnostic.

Morphology and 3D reconstruction

Clade III is relatively easy to distinguish from the other two clades because of its irregular undulation in the posterior edge of the cephalic capsule. These undulations can be more or less pronounced. Additionally, the amphid fovea is not completely surrounded by the cephalic capsule in clade III whereas it is in clades I and II (Fig. 5). This last character is more constant and reliable than the undulation in the posterior edge of the cephalic capsule. As the cephalic capsule length was amongst the three most important characters (excluding sexual characters) to distinguish the three clades, a 3D reconstruction was made. This showed that clade III possessed two subdorsal tropis-like projections in the internal wall of the cephalic capsule at the dorsal tooth level although it does not extend as far anteriorly as the ventral tropis (Figs 6, 7).

DISCUSSION

Our data show that *T. trachygaster* is actually a species complex containing at least three molecularly and morphologically distinct species. For the mitochondrial COI gene, the minimum genetic divergences between clades always exceeded the threshold level of interspecific divergence proposed for parasitic (Ferri *et al*., 2009) and marine (Derycke *et al*., 2010b) nematodes. In view of the possibility of heteroplasmy (Tigano *et al*., 2005) or pseudogenes (Song *et al*., 2008) there is a need to use more than one molecular marker to delimit species. The 28S and ITS regions have been widely used to delineate nematode species (Powers *et al*., 1997; Litvaitis *et al*., 2000; Nguyen, Maruniak & Adams, 2001), but they may be less suitable to distinguish closely related species (Fonseca *et al*., 2008). Our data and those of Derycke *et al*. (2010a) show that the minimum genetic divergence amongst the *Thoracostoma* clades was very low for the D2D3 region (0.7–1.0%), and between 3.4–6.9% for the ITS region. This indicates that ITS is more suitable than D2D3 to adequately delineate closely related species. Both nuclear markers clearly support the mitochondrial tree topology and suggest that the three clades are distinct phylogenetic entities.

Our morphological data also support the separation of specimens into three groups, although no single diagnostic feature was able to morphologically distinguish all three cryptic species. This is in agreement with previous morphological studies of cryptic marine nematode species complexes (Derycke *et al*., 2008a; Fonseca *et al*., 2008). Clade III is generally shorter in body length than the other two clades, but there is so much variation that it cannot be used as a quantitative character. The undulation in the posterior edge of the cephalic capsule of clade III is similar to that in *T. microlobatum* Hope, 1967. However, clade III specimens are much smaller than *T. microlobatum* (4–5.5 mm clade III vs. 9.4–20.4 mm *T. microlobatum*), and do not have a granulous ring surrounding the stoma. Clade III also resembles *Thoracostoma zolae* Marion, 1870 but the females of clade III have the vulva surrounded by intracuticular granules and males have winged precloacal supplements. Very

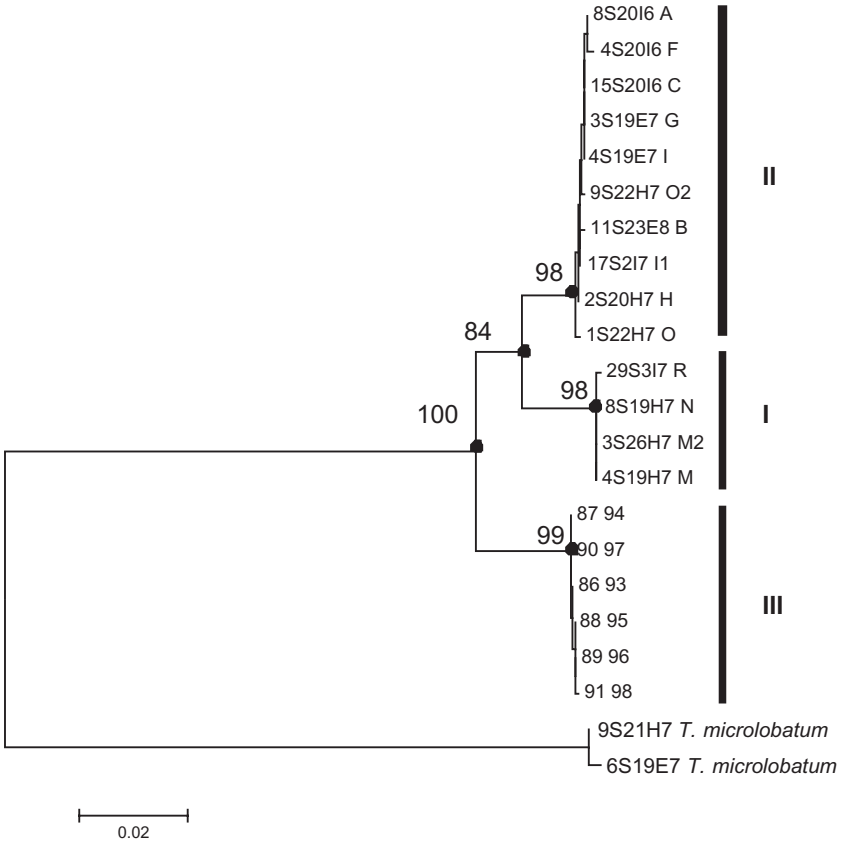

Figure 3. The nuclear D2D3 region of the 28S rDNA and internal transcribed spacer concatenated neighbour-joining tree based on P-distances with specimens from 2007 and from the new clade III (represented by numbers) from 2009 and 2010. The bootstrap values are indicated on the branches.

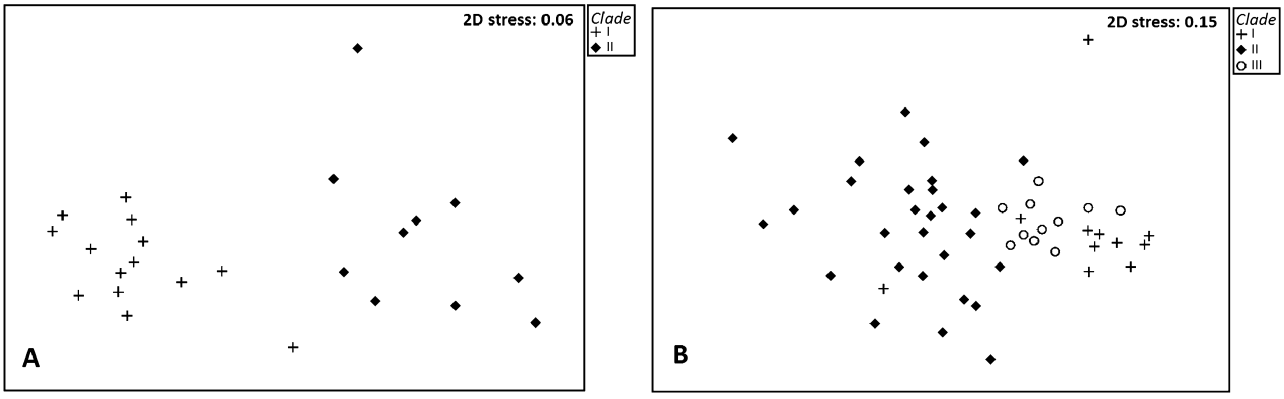

Figure 4. A, nonmetric multidimensional scaling (MDS) comparing video-measured individuals from clades I and II found in 2007. B, nonmetric MDS comparing directly measured individuals from slides from clades I, II, and III found in 2009 and 2010 including sexual characters (males only).

Table 3. Minimum, maximum, and mean values (in μm) of the nonsexual characters of clades I, II, and III of the *Thoracostoma trachygaster* complex along the California coast

	Clade I			Clade II			Clade III			Holotype Hope (1967)
Character	Min.	Max.	Mean	Min.	Max.	Mean	Min.	Max.	Mean	Absolute values
Nematode length	3906	5908	4743	4607	9841	6469	4093	5890	5252	6280
Pharynx length	774	1053	901	735	1508	1116	957	1144	1032	–
Nerve ring distance anterior end	261	333	291	230	514	366	301	357	329	–
Ocelli distance anterior end	59	85	72	69	120	93	58	84	73	106
cbd of the base pharynx	95	158	114	104	201	161	132	166	146	–
mbd	120	172	133	134	220	184	139	204	159	–
abd	77	102	86	98	145	124	87	120	99	84
Tail length	60	100	81	82	132	108	62	90	80	78
Amphid length	8	11	9	8	13	11	7	11	9	8
Amphid width fovea	5	8	7	6	11	8	6	8	7	7
Amphid open distance anterior end	10	19	15	13	24	18	13	19	17	15
cbd base cephalic capsule	37	59	44	53	67	59	46	56	51	55
Cephalic capsule width posterior edge	32	45	37	42	55	47	41	47	44	42
Cephalic capsule width anterior edge	19	29	21	19	33	28	21	27	24	25
Cephalic capsule length	16	27	22	22	43	30	25	31	27	36
Tropis length	9	13	11	10	16	13	9	16	12	12

Measurements obtained from Hope's original description have also been added.
Abbreviations: abd, anal body diameter; cbd, corresponding body diameter; Max., maximum; mbd, maximum body diameter; Min., minimum.

Table 4. Minimum, maximum, and mean values (in μm) of the measured sexual characters of clades I, II, and III of the *Thoracostoma trachygaster* complex along the California coast

	Clade I			Clade II			Clade III			Holotype Hope (1967)
Character	Min.	Max.	Mean	Min.	Max.	Mean	Min.	Max.	Mean	Absolute values
Gubernaculum length	28	48	37	39	75	55	38	64	47	–
Apophysis length	20	26	24	25	47	37	20	41	27	–
Spicule length	101	125	116	124	173	154	103	169	124	138
Distance from supplement to cloaca	54	107	73	89	132	107	78	92	87	76

Measurements obtained from Hope's original description have also been added.
Max., maximum; Min., minimum.

Figure 5. Head and tail regions of clades I, II, and III. A, B, clade I; C, D, clade II; E, F, clade III.

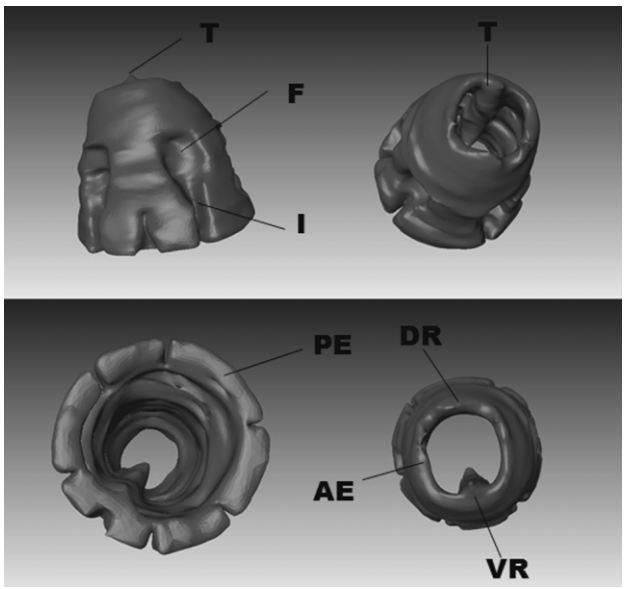

Figure 6. 3D reconstruction of the cephalic capsule of clade II. Abbreviations: AE, anterior edge; DR, dorsal region; F, fenestra; I, incision; PE, posterior edge regular; T, tropis; VR, ventral region.

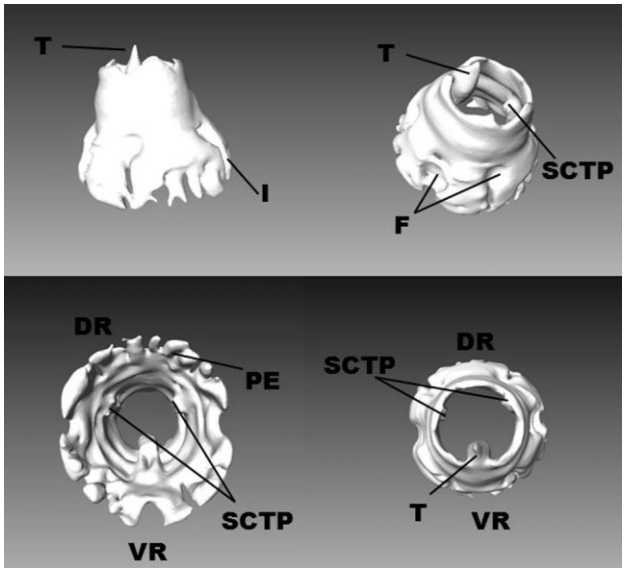

Figure 7. 3D reconstruction of the cephalic capsule of clade III. Abbreviations: AE, anterior edge; DR, dorsal region; F, fenestra; I, incision; PE, posterior edge irregular; SCTP, subdorsal cephalic tropis-like projections that are not present in clade II; T, tropis; VR, ventral region.

accurate 3D reconstruction usually requires transmission electron microscopy (TEM) data (Bumbarger *et al*., 2007; Ragsdale *et al*., 2008). In this study we used conventional light microscopy, which provides a less detailed view of the structures. Nevertheless, the 3D view clearly showed that clade III specimens have two subdorsal cylindrical tropis-like projections in the middle of the cephalic capsule at the level of the dorsal tooth, similar to the ventral tropis but not extending until the posterior edge of the cephalic capsule as is found with the subdorsal tropes of *T. microlobatum*. Additionally, COI sequence divergence between clade III and *T. microlobatum* was above 24%, supporting the hypothesis that they are distinct species.

Although our results show that a combination of characters permitted us to distinguish cryptic species, the significant differences between measurements from the videos and from the microscopic slides illustrate the impact of the method used and the necessity to provide this information for correct interpretation of morphological variation, especially when species are identified solely based on slight difference in morphometrics. These morphometric differences may be the result of different measurement methods, different taxonomists using different microscopes or, alternatively, intraspecific variation (e.g. food availability may also affect morphometric variation, Schiemer, 1982; Herman & Vranken, 1988). Our study demonstrates that the effect of these confounding factors can be overcome by using an integrative approach for delineating species.

Comparing our data with the measurements of the holotype of *T. trachygaster* (Tables 3, 4), the lack of the tropis-like projections in the cephalic capsule in the holotype and the fact that clade II was the most abundant clade in similar localities collected by Hope (1967) such as Pebble beach near Torrey Pines, suggest that clade II is *T. trachygaster*. In view of the sympatric distribution of the clades and of the wide ranges of the measurements of Hope's paratypes, these paratypes most likely belong to more than one clade. As all specimens have been used for molecular analyses, our holotypes consist of partial specimens: we have deposited permanent slides of head, tail, and vulva sections of each clade in the Royal Belgian Institute of Natural Sciences and in the Zoology Museum of Ghent University (Belgium), along with DNA material. The description of the new *Thoracostoma* species is given in the Appendix.

Thoracostoma igniferum sp. nov. (clade III) was found in the most northerly sampled beach, where it co-occurred with *T. trachygaster* (clade II) and *T. fatimae* sp. nov. (clade I). In Huntington Beach, only *T. trachygaster* was present at the two time points (2007 and 2009), but in Malibu Beach and Torrey Pines Beach, *T. trachygaster* and *T. fatimae* co-occurred and fluctuated in their abundances over time. Temporal fluctuations in the abundance of genetically distinct species were already observed in previous work (Derycke *et al*., 2006, 2007a), but our results now indicate that this unrecognized diversity

is also present in species with quite distinct life history characteristics from those of the rhabditid and monhysterid species previously studied. This further supports the contention that nematode diversity may be seriously underestimated. Allopatric speciation has been put forward as the most likely driver of cryptic speciation in the rhabditid species complex (Derycke *et al*., 2008b). We have currently insufficient data to hypothesize whether this would also be the case for the *T. trachygaster* complex.

CONCLUSION

The integrative approach allowed us to find morphological differences amongst genetic lineages within what was previously thought to be one nominal species. By describing these new species and giving them scientific names, we have ensured that these closely related species are no longer cryptic. This is important for a wide range of future studies addressing biogeography, biodiversity, phylogeography, and population genetics of nematodes in general, and *Thoracostoma* in particular.

ACKNOWLEDGEMENTS

This research was financially supported by the VLIR-UOS, the Flemish Fund for Scientific Research (F.W.O.) through project 3G040407 and through research grant 1507709, and by Ghent University through the BOF project B/07778/02. S. D. acknowledges a postdoctoral fellowship from the F.W.O. We are very grateful for the valuable help of Annelien Rigaux (sequencing), and Dr Maxime Willems (3D reconstruction). The use of the AMIRA software was courtesy of Prof. Dr Dominique Adriaens.

REFERENCES

Abebe E, Grizzle RE, Hope D, Thomas, WK 2004. Nematode diversity in the Gulf of Maine, USA, and a Web-accessible, relational database. *Journal of the Marine Biological Association of the UK* **84:** 1159–1167.

Adams BJ. 2001. The species delimitation uncertainty principle. *Journal of Nematology* **33:** 153–160.

Bickford D, Lohman DJ, Sodhi NS, Peter KL, Ng PKL, Rudolf Meier R, Winker K, Ingram KK, Das I. 2007. Cryptic species as a window on diversity and conservation. *Trends in Ecology & Evolution* **22:** 148–155.

Bumbarger DJ, Crum J, Ellisman MH, Baldwin JG. 2007. Three-dimensional fine structural reconstruction of the nose sensory structures of *Acrobeles complexus* compared to *Caenorhabditis elegans* (Nematoda: Rhabditida). *Journal of Morphology* **268:** 649–663.

Clarke KR, Gorley RN. 2006. *PRIMER v6: user manual/tutorial*. Plymouth: PRIMER-E.

Coomans A. 2002. Present status and future of nematode systematics. *Nematology* **4:** 573–582.

De Ley P, Bert W. 2002. Video capture and editing as a tool for the storage, distribution and illustration of morphological characters of nematodes. *Journal of Nematology* **34:** 296–302.

De Ley P, De Ley IT, Morris K, Abebe E, Mundo-Ocampo M, Yoder M, Heras J, Waumann D, Rocha-Olivares A, Burr AHJ, Baldwin JG, Thomas WT. 2005. An integrated approach to fast and informative morphological vouchering of nematodes for applications in molecular barcoding. *Philosophical Transactions of the Royal Society of London. Series B, Biological sciences* **360:** 1945–1958.

De Ley P, Félix MA, Frisse LM, Nadler SA, Sternberg PW, Thomas WK. 1999. Molecular and morphological characterization of two reproductively isolated species with mirror-image anatomy (Nematoda: Cephalobidae). *Nematology* **1:** 591–612.

Derycke S, Backeljau T, Vlaeminck C, Vierstraete A, Vanfleteren J, Vincx M, Moens T. 2006. Seasonal dynamics of population genetic structure in cryptic taxa of the Pellioditis marina complex (Nematoda: Rhabditida). *Genetica* **128:** 307–321.

Derycke S, Backeljau T, Vlaeminck C, Vierstraete A, Vanfleteren J, Vincx M, Moens T. 2007a. Spatiotemporal analysis of population genetic structure in *Geomonhystera disjuncta* (Nematoda, Monhysteridae) reveals high levels of molecular diversity. *Marine Biology* **151:** 1799–1812.

Derycke S, De Ley P, De Ley IT, Holovachov O, Rigaux A, Moens T. 2010a. Linking DNA sequences to morphology: cryptic diversity and population genetic structure in the marine nematode *Thoracostoma trachygaster* (Nematoda, Leptosomatidae). *Zoologica Scripta* **39:** 276–289.

Derycke S, Fonseca G, Vierstraete A, Vanfleteren J, Vincx M, Moens T. 2008a. Disentangling taxonomy within the *Rhabditis* (*Pellioditis*) *marina* (Nematoda, Rhabditidae) species complex using molecular and morphological tools. *Zoological Journal of the Linnean Society* **152:** 1–15.

Derycke S, Remerie T, Backeljau T, Vierstraete A, Vanfleteren J, Vincx M, Moens T. 2008b. Phylogeography of the *Rhabditis* (*Pellioditis*) *marina* species complex: evidence for long-distance dispersal, and for range expansions and restricted gene flow in the northeast Atlantic. *Molecular Ecology* **17:** 3306–3322.

Derycke S, Remerie T, Vierstraete A, Backeljau T, Vanfleteren J, Vincx M, Moens T. 2005. Mitochondrial DNA variation and cryptic speciation within the free-living marine nematode *Pellioditis marina*. *Marine Ecology-Progress Series* **300:** 91–103.

Derycke S, Vanaverbeke J, Rigaux A, Backeljau T, Moens T. 2010b. Exploring the use of cytochrome oxidase c subunit 1 (COI) for DNA barcoding of free-living marine nematodes. *PLoS ONE* **5:** e13716. DOI: 10.1371/journal.pone.0013716.

Dolphin K, Belshaw R, Orme CDL, Quicke DLJ. 2000. Noise and incongruence: interpreting results of the incongruence length difference test. *Molecular Phylogenetics and Evolution* **17:** 401–406.

Edison AS. 2009. *Caenorhabditis elegans* pheromones regulate multiple complex behaviors. *Current Opinion in Neurobiology* **19:** 378–388.

Ferri E, Barbuto M, Bain O, Galimberti A, Uni S, Guerrero R, Ferté H, Bandi C, Martin C, Casiraghi M. 2009. Integrated taxonomy: traditional approach and DNA barcoding for the identification of filarioid worms and related parasites (Nematoda). *Frontiers in Zoology* **6:** 1–12.

Filipjev IN. 1916. Free-living nematodes in the collection of the Zoological Museum of the Imperial Academy of Sciences in Petrograd. *Ezhegodnik Zoologicheskogo Muzeia Imperatorskoi Akademii Nauk* **2:** 159–116.

Floyd R, Abebe E, Papert A, Blaxter M. 2002. Molecular barcodes for soil nematodes identification. *Molecular Ecology* **11:** 839–850.

Fonseca G, Derycke S, Moens T. 2008. Integrative taxonomy in two free-living nematode species complex. *Biological Journal of the Linnean Society* **94:** 737–753.

Galtier N, Gouy M, Gautier C. 1996. SEAVIEW and PHYLO_WIN: two graphic tools for sequence alignment and molecular phylogeny. *Computer Applications in the Biosciences* **12:** 543–548.

Goetze E, Kiørboe T. 2008. Heterospecific mating and species recognition in the planktonic marine copepods *Temora longicornis* and *Temora stylifera*. *Marine Ecology Progress Series* **370:** 185–198.

Gozel U, Lamberti F, Duncan L, Agostinelli A, Rosso L, Nguyen K, Adams BJ. 2006. Molecular and morphological consilience in the characterisation and delimitation of five nematode species from Florida belonging to the *Xiphinema americanum*-group. *Nematology* **8:** 521–532.

Harmon LJ, Matthews B, Des Roches S, Chase JM, Shurin JB, Schluter D. 2009. Evolutionary diversification in stickleback affects ecosystem functioning. *Nature* **458:** 1167–1170.

Herman PMJ, Vranken G. 1988. Studies of the life-history and energetics of marine and brackish-water nematodes. II: production, respiration and food uptake by Monhystera *disjuncta*. *Oecologia* **77:** 457–463.

Holovachov O, Boström S, Mundo-Ocampo M, De Ley IT, Yoder M, Burr AHJ, De Ley P. 2009. Morphology, molecular characterization and systematic position of *Hemiplectus muscorum* Zell, 1991 (Nematoda: Plectida). *Nematology* **11:** 719–737.

Hope WD. 1967. Free-living marine nematodes of the genera *Pseudocella* Filipjev, 1927, *Thoracostoma* Marion, 1870, and *Deontostoma* Filipjev, 1916 (Nematoda: Leptosomatidae) from the West Coast of North America. *Transactions of the American Microscopical Society* **86:** 307–334.

Hugot JP, Baujard P, Morand S. 2001. Biodiversity in helminths and nematodes as a field of study: an overview. *Nematology* **3:** 199–208.

Kiontke K, Fitch DHA. 2010. Phenotypic plasticity: different teeth for different feasts. *Current Biology* **20:** R710–R712.

Knowlton N. 2000. Molecular genetic analyses of species boundaries in the sea. *Hydrobiologia* **420:** 73–90.

Lambshead PJD. 2001. Marine nematode diversity. In: Chen ZX, Chen SY, Dickson DW, eds. *Nematology, advances and perspectives*. San Francisco, CA: ACSE-TUP Book Series, 436–467.

Litvaitis MK, Bates JW, Hope WD, Moens T. 2000. Inferring a classification of the Adenophorea (Nematoda) from nucleotide sequences of the D3 expansion segment (26/28S rDNA). *Canadian Journal of Zoology* **78:** 911–922.

Mawson PM. 1958. Free-living nematodes. Section 3: Enoploidea from subantarctic stations B.A.N.Z. *Antarctic Research Expedition Reports, Series B* **6:** 307–358.

Nadler SA. 2002. Species delimitation and nematodes biodiversity: phylogenies rule. *Nematology* **4:** 615–625.

Neres PF, Fonseca-Genevois VG, Torres RA, Cavalcanti MF, Castro FJV, Silva NRR, Rieger TT, Decraemer W. 2010. Morphological and molecular taxonomy of a new *Daptonema* (Nematoda, Xyalidae) with comments on the systematics of some related taxa. *Zoological Journal of the Linnean Society* **158:** 1–15.

Nguyen KB, Maruniak J, Adams BJ. 2001. Diagnostic and phylogenetic utility of the rDNA internal transcribed spacer sequences of Steinernema. *Journal of Nematology* **33:** 73–82.

Nygren A, Eklöf J, Pleijel F. 2010. Cryptic species of *Notophyllum* (Polychaeta: Phyllodocidae) in Scandinavian waters. *Organisms Diversity & Evolution* **10:** 193–204.

O'Halloran DM, Fitzpatrick DA, Burnell AM. 2006. The chemosensory system of *Caenorhabditis elegans* and other nematodes. In: Dicke M, Takken W, eds. *Chemical ecology: from gene to ecosystem*. Dordrecht: Springer, 71–88.

Pereira TJ, Fonseca G, Mundo-Ocampo M, Guilherme BC, Rocha-Olivares A. 2010. Diversity of free-living marine nematodes (Enoplida) from Baja California assessed by integrative taxonomy. *Marine Biology* **157:** 1665–1678.

Powers T. 2004. Nematode molecular diagnostics: from bands to barcodes. *Annual Review of Phytopathology* **42:** 367–383.

Powers TO, Todd TC, Burnell AM, Murray PCB, Fleming CC, Szalanski AL, Adams BA, Harris TS. 1997. The internal transcribed spacer region as a taxonomic marker for nematodes. *Journal of Nematology* **29:** 441–450.

Ragsdale EJ, Crum J, Ellisman MH, Baldwin JG. 2008. Three-dimensional reconstruction of the stomatostylet and anterior epidermis in the nematode *Aphelenchus avenae* (Nematoda: Aphelenchidae) with implications for the evolution of plant parasitism. *Journal of Morphology* **269:** 1181–1196.

Sanderson MJ, Shaffer HB. 2002. Troubleshooting molecular phylogenetic analyses. *Annual Review of Ecology and Systematics* **33:** 49–72.

Schiemer F. 1982. Food dependence and energetics of free-living nematodes. I. Respiration, growth and reproduction of *Caenorhabditis briggsae* (Nematoda) at different levels of food supply. *Oecologia* **54:** 108–121.

Song H, Buhay JE, Whiting MF, Crandall KA. 2008. Many species in one: DNA barcoding overestimates the number of species when nuclear mitochondrial pseudogenes are coamplified. *Proceedings of the National Academy of Sciences, USA* **105:** 13486–13491.

StatSoft, Inc. 2004. STATISTICA (data analysis software system), version 7. http://www.statsoft.com

Suatoni E, Vicario S, Riceb S, Snell T, Caccone A. 2006. An analysis of species boundaries and biogeographic patterns in a cryptic species complex: the rotifer–*Brachionus plicatilis*. *Molecular Phylogenetics and Evolution* **41:** 86–98.

Swofford DL. 1998. *PAUP*. Phylogenetic analysis using parsimony (*and other methods), version 4*. Sunderland, MA: Sinauer & Associates.

Tamura K, Dudley J, Nei M, Kumar S. 2007. MEGA4: Molecular Evolutionary Genetics Analysis (MEGA) software version 4.0. *Molecular Biology and Evolution* **24:** 1596–1599.

Tandingan De Ley L, Mundo-Ocampo M, Yoder M, De Ley P. 2007. Nematodes from vernal pools in the Santa Rosa Plateau Ecological Reserve, California I. *Hirschmanniella santarosae* sp. n. (Nematoda: Pratylenchidae), a cryptic sibling species of *H. pomponiensis* Abdel-Rahman & Maggenti, 1987. *Nematology* **9:** 405–429.

Tigano MS, Carneiro RMDG, Jeyaprakash A, Dickson DW, Adams B. 2005. Phylogeny of *Meloidogyne* spp. Based on 18S rDNA and the intergenetic region of mitochondrial DNA sequences. *Nematology* **7:** 851–862.

Wiens JJ, Penkrot TA. 2002. Delimiting species using DNA and morphological variation and discordant species limits in spiny lizards (*Sceloporus*). *Systematic Biology* **51:** 69–91.

Wieser W. 1956. Some free-living marine nematodes. *Galathea* **2:** 243–253.

Yoder M, De Ley IT, King I, Mundo-Ocampo M, Mann J, Blaxter M, Poiras L, De Ley P. 2006. DESS: A versatile solution for preserving morphology and DNA of nematodes. *Journal of Nematology* **38:** 302.

APPENDIX

DESCRIPTION OF *THORACOSTOMA FATIMAE* AND *THORACOSTOMA IGNIFERUM*

All specimens were fixed and preserved in DESS. They were subsequently mounted on temporary slides containing a droplet of sterile water (without transformation through glycerine, because we wanted to obtain DNA material from the same individuals), measured, and photographed digitally (see Material and methods). Specimens were then taken out of the slide, and head, tail, or in the case of females the vulva, regions were cut and preserved in DESS. For the type material, these regions were transferred through glycerine and mounted in permanent slides.

***THORACOSTOMA FATIMAE* SP. NOV.** (CLADE I) (FIG. 8A–D, TABLE 5)

Diagnosis: Thoracostoma fatimae sp. nov. is morphologically nearly identical to *Thoracostoma trachygaster* but can be distinguished from the latter by spicule length (100–123 μm in *T. fatimae* sp. nov. vs. 124–173 μm in *T. trachygaster* in the current study). The new species also closely resembles *T. igniferum* sp. nov., the second new species described in this contribution, but can be clearly differentiated by the cephalic capsule, without irregular undulations as in *T. igniferum* sp. nov. *Thoracostoma fatimae* sp. nov., although morphologically very similar to *T. trachygaster*, was supported as a valid taxon by molecular analyses. Phylogenetic trees based on nuclear and mitochondrial markers showed it to be genetically more closely related to *T. trachygaster* than to *T. igniferum*. The I3M11 mitochondrial cytochrome oxidase c subunit I (COI) sequences of *T. fatimae* are 5.7–8.2% divergent from those of *T. trachygaster*, and 9.0–10.1% divergent from those of *T. igniferum*. Nuclear internal transcribed spacer (ITS) sequence divergence ranges between 3.4–3.7% with *T. trachygaster*, and between 6.7–6.9% with *T. igniferum*. Divergence ranges of the nuclear D2D3 sequences of the 28S rDNA were small (0.7–1.0 and 0.8–1.0%, respectively).

Etymology: The new species is a homage to my mother Fátima Oliveira, who provided substantial emotional support during this study.

Specimens: Eighteen (16 males, two females).

Type material: Holotype: 3D31E10 (male). Paratypes 1D31E10 and 2D31E10 (two males), and 4D31E10 (female), along with the holotype are deposited in the Royal Belgian Institute of Natural Science (RBINS) – Brussels, under the numbers RIT780 (holotype), RIT781-RIT783 (paratypes). Paratypes 4D18C10 and 6D25C10 (two males) and 7D25E10 (female) are deposited in the Zoology Museum of Ghent University, under the numbers UGMD104117–UGMD104119. DNA material of the seven specimens is available in the Zoology Museum of Ghent University, under the numbers UGMD125000–UGMD125006. DNA sequences of *T. fatimae* specimens that were video vouchered (Derycke *et al*., 2010a) are available in GenBank under the accession numbers FN433782, FN433787, FN433788, FN433790, FN433799, FN433803–FN433806 (COI), FN433920–FN433921 (ITS), FN433908, FN433911 (D2D3). COI accession numbers of specimens 4D18C10, 6D25C10, 1D31E10, and 7D25E10 are FR853137–FR853140.

Description: Body long, largely cylindrical, neck region anteriorly tapered, tail short i.e. about one anal body width long, dorsally convex and posterior end blunt, rounded. Posterior body region ventrally curved upon fixation, more pronounced in male com-

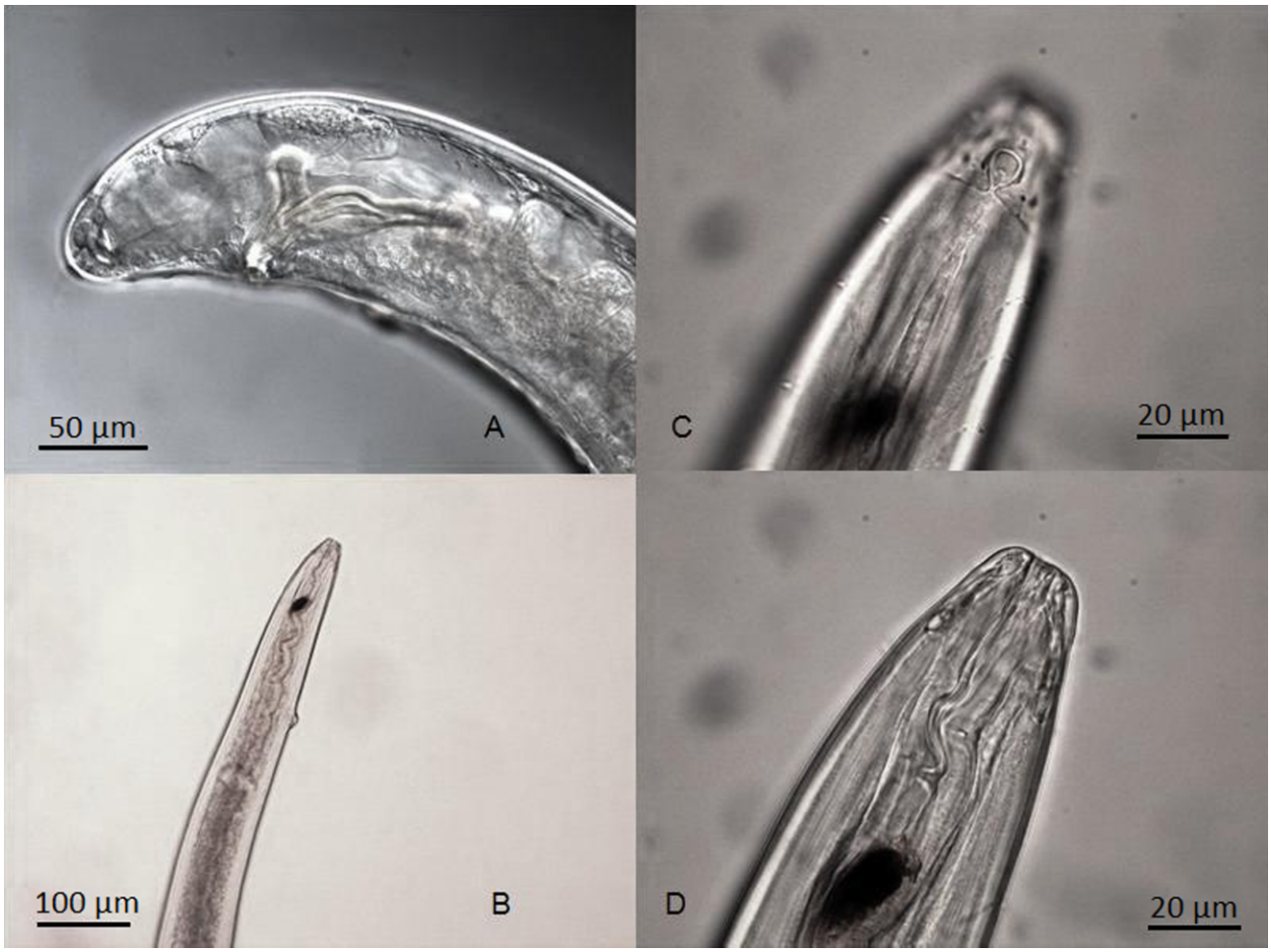

Figure 8. Morphology of ***Thoracostoma fatimae*** **sp. nov.** Pictures are from the holotype. A, tail region with spicules (SP), gubernaculums (GU), apophysis (AP), and ventromedian precloacal supplement (PS); B, anterior region with ocelli (ES) and nerve ring (NR); C, head region with a well-developed cephalic capsule (PCC), amphid (AM), and cephalic setae (CS); D, cephalic capsule at middle level with the ventral tropis (T).

pared to female. Obvious eyespots present on both sides anteriorly in neck region i.e. at two to four times lip region width from anterior end. Cuticle appearing smooth but with very fine transversal striation visible in head region. In males, cuticle with rugose appearance in ventral region from cloaca extending until the anterior-most subventral setiform supplement. Lip region with six lips, anterior sensilla arranged in two crowns (pattern 6 + 10). Inner labial sensilla of the anterior-most crown papilliform and outer labial sensilla and cephalic sensilla of the posterior crown setiform (2–4 µm long). Cervical setae arranged in six rows, with visible sensillar canal and dendritic processes between the cephalic capsule suture and eyespot. Cephalic capsule well developed, with slightly marked anterior lobes except for the ventral tropis orientated to the anterior end. Posterior border capsule divided into six lobes by narrow incisions through which pass the innervations of the anterior sensilla and amphids; incisions ending in circular fenestrae, showing some slight variation in shape. Amphidial fovea shield-shaped to circular. Buccal cavity with a short blunt dorsal tooth. Pharynx without bulbus and with nerve ring located about one third of the total pharynx length from anterior end. Cardia triangular in longitudinal optical section, projecting into intestinal lumen. Three caudal glands, extending anteriorly beyond the rectum.

Males: Reproductive system diorchic, posterior testis reflexed. Precloacal ventral body wall appearing rugose because of numerous minute protuberances extending more or less until the anterior-most setiform subventral copulatory supplements arranged in a longitudinal series. Single ventromedian copulatory supplement cyathiform and winged. Spicules, ventrally curved with mid-blade portion widened.

Table 5. Morphometric data of ***Thoracostoma fatimae* sp. nov.** individuals (in μm)

Character	3D31E10 (m)	1D11C10 (m)	2D11C10 (m)	1D12C10 (m)	4D12C10 (m)	1D18C10 (m)	2D18C10 (m)	4D18C10 (m)	3D24C10 (m)	4D24C10 (m)	6D24C10 (m)	1D25C10 (m)	1D25E10 (m)
Nematode length	4344	5473	5598	6314	5908	4954	5881	6112	5176	4795	4599	4402	4618
Pharynx length	829	1053	1048	1096	967	968	1003	1079	998	1021	920	885	846
Nerve ring distance anterior end	284	313	310	353	290	316	303	323	331	333	291	307	275
Eyespot distance anterior end	71	75	76	80	85	73	75	74	85	80	73	131	–
cbd at the base of pharynx	100	111	104	154	143	98	131	127	115	119	106	208	134
mbd	124	131	135	167	172	126	144	145	134	137	109	224	146
abd	82	86	97	127	102	87	80	105	89	–	83	87	87
Tail length	80	84	84	114	94	74	87	82	85	75	66	70	85
Amphid length	9	8	8	13	9	9	10	8	9	9	9	10	9
Amphid aperture	6	8	6	10	7	7	7	8	8	7	6	6	6
Amphid aperture distance to anterior end	16	14	15	19	19	16	16	13	16	16	16	16	15
cbd at base cephalic capsule	42	41	43	67	52	42	41	53	42	51	48	43	42
Cephalic capsule width posterior edge	34	35	33	55	44	34	35	44	35	43	38	38	34
Cephalic capsule width anterior edge	21	19	22	30	25	19	19	20	21	22	20	18	23
Cephalic capsule length	24	22	22	30	24	25	23	22	22	22	23	22	18
Tropis length	10	10	11	14	11	9	11	8	12	10	11	10	13
a	35	42	41	38	34	39	41	42	39	35	42	20	32
b	5	5	5	6	6	5	6	6	5	5	5	5	5
c	54	65	66	55	63	67	67	74	61	64	70	63	54

Character	2D25E10 (m)	3D25E10 (m)	5D25E10 (m)	6D25E10 (m)	7D25E10 (f)	8D25E10 (f)	1D31E10 (m)	2D31E10 (m)	4D31E10 (f)	5D31E10 (m)	Min.	Max.	Mean	SD
Nematode length	3906	3986	4540	3947	4374	4105	4976	4414	4403	4227	3906	6314	4850	738
Pharynx length	830	862	894	845	882	774	843	867	850	824	774	1096	925	94
Nerve ring distance anterior end	280	268	290	287	283	273	261	280	301	274	261	353	297	24
Eyespot distance anterior end	67	66	72	67	67	61	69	59	76	65	59	131	75	14
cbd at the base of pharynx	110	101	106	99	111	121	103	95	114	101	95	208	119	25
mbd	127	–	121	127	121	138	120	123	129	127	109	224	138	25
abd	84	77	87	84	78	86	80	83	80	92	77	127	89	11
Tail length	88	60	86	78	75	91	73	80	63	100	60	114	82	12
Amphid length	8	8	9	7	9	8	9	9	11	10	7	13	9	1
Amphid aperture	6	7	8	5	6	6	7	7	8	8	5	10	7	1
Amphid aperture distance to anterior end	17	14	15	14	11	15	12	9	13	16	9	19	15	2
cbd at base cephalic capsule	46	42	42	37	43	49	46	40	43	43	37	67	45	6
Cephalic capsule width posterior edge	39	35	38	32	35	38	37	33	35	32	32	55	37	5
Cephalic capsule width anterior edge	22	21	21	20	21	21	24	19	21	19	18	30	21	3
Cephalic capsule length	24	19	24	16	18	24	20	21	23	22	16	30	22	3
Tropis length	9	11	9	9	10	11	10	9	11	11	8	14	11	1
a	31	–	38	31	36	30	41	36	34	33	20	42	36	5
b	5	5	5	5	5	5	6	5	5	5	5	6	5	0
c	44	67	53	50	58	45	68	55	70	42	42	74	60	9

The individuals are indicated by the voucher code. The first individual (3D31E10) is the holotype.
Abbreviations: a, body length/body width; abd, anal body diameter; b, body length/pharynx length; c, body length/tail length; cbd, corresponding body diameter; f, female; m, male; Max., maximum; mbd, maximum body diameter; Min., minimum.

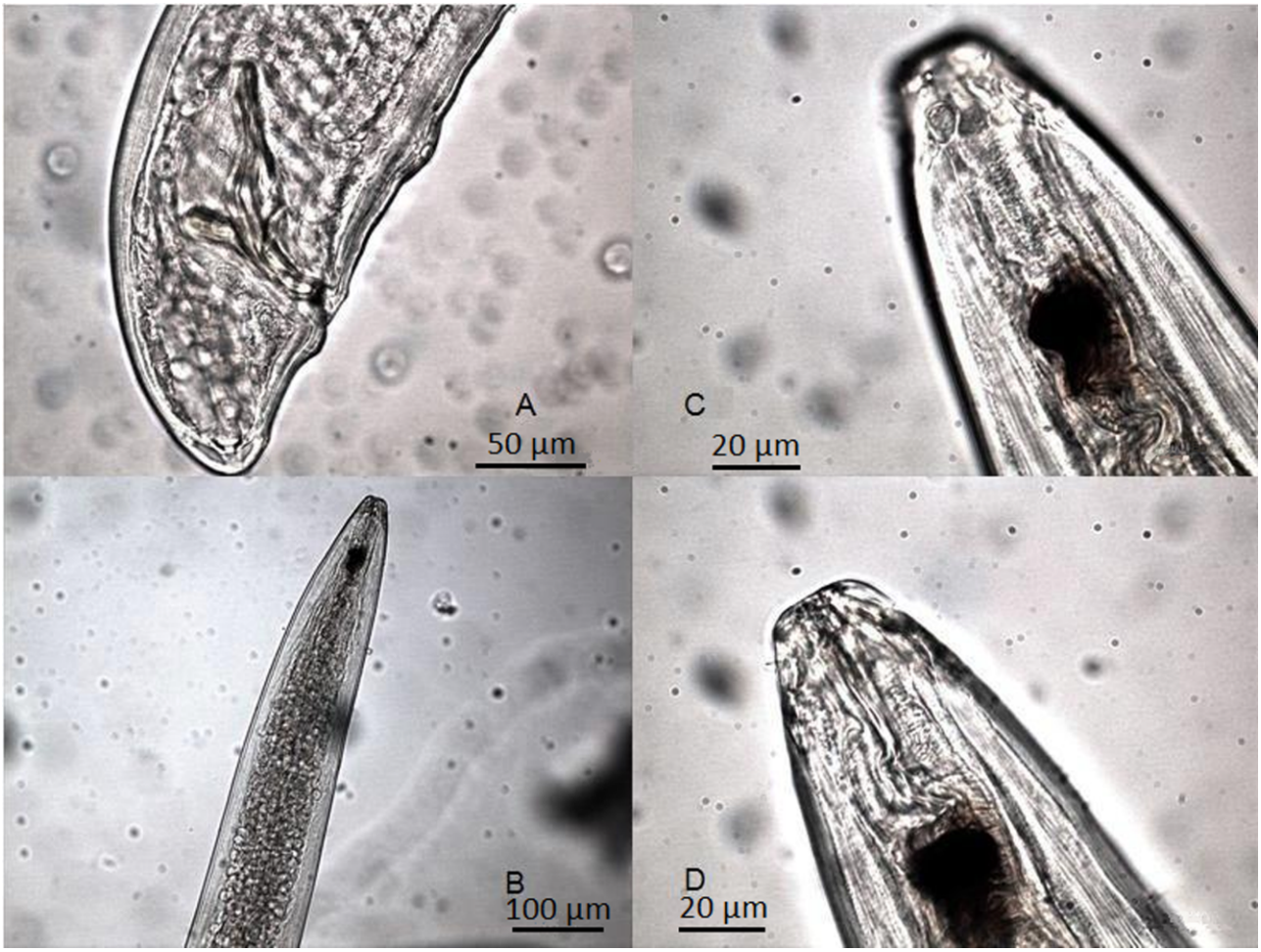

Figure 9. Morphology of ***Thoracostoma igniferum* sp. nov.**, pictures are from the holotype. A, tail region with spicules (SP), gubernaculums (GU), apophysis (AP), and ventromedian precloacal supplement (PS); B, anterior region with ocelli (ES) and nerve ring (NR); C, head region with a well-developed cephalic capsule with irregular undulations of the posterior edge (PCC) and amphid (AM); D, cephalic capsule at middle level with the ventral tropis (T).

Gubernaculum with two apophyses and the crura with membrane embracing the spicule.

Female: Reproductive system didelphic, amphidelphic, with reflexed ovaries. Vulva, a transverse slit in ventral view, surrounded by a punctuated cuticle and located at 62% of total body length from anterior end.

Type locality: Holotype collected from stranded holdfasts of *Macrocystis* sp. in Malibu Beach, California, USA. Additional locations where specimens were collected are Ventura Beach and Torrey Pines, California, USA.

THORACOSTOMA IGNIFERUM SP. NOV. (CLADE III) (FIG. 9A–D, TABLE 6)

Diagnosis: Thoracostoma igniferum sp. nov. closely resembles *T. trachygaster* and *T. fatimae* sp. nov. but can be distinguished from both by the irregular posterior edge of the cephalic capsule and the two internal subdorsal tropis-like projections in the wall of the cephalic capsule (only visible in cross-section). DNA sequences of the mitochondrial COI gene and the nuclear ITS and D2D3 regions differ from those of *T. trachygaster* in 10.9–13.3, 5.2–5.5, and 1.0–1.1%, respectively, and from those of *T. fatimae* in 9.0–10.9, 6.7–6.9, and 0.8–1.0%, respectively.

Etymology: The name refers to the Latin word 'ignis', which means fire. It refers to the irregular undulations in the posterior edge of the cephalic capsule, which resemble flames.

Specimens: Eleven (eight males, three females)

Type material: Holotype 2D24C10 (male). Paratypes 2D12C10 (female), 3D18C10 and 5D12C10 (males), and the holotype deposited in the Royal Belgian

Table 6. Morphometric data of ***Thoracostoma igniferum* sp. nov.** individuals (in μm)

Character	2D24C10 (m)	2D12C10 (f)	3D12C10 (m)	5D12C10 (m)	6D12C10 (f)	1D13C10 (m)	3D13C10 (f)	3D18C10 (m)	1D24C10 (m)	5D24C10 (m)	2D25C10 (m)	Min.	Max.	Mean	SD
Nematode length	4907	5652	5615	5242	5502	5890	5350	5241	4966	4093	5312	4093	5890	5286	493
Pharynx length	978	1144	1030	996	1064	1063	1031	1048	1072	957	973	957	1144	1038	54
Nerve ring distance anterior end	310	355	301	338	335	329	326	316	357	354	302	301	357	331	20
Eyespot distance anterior end	58	80	77	72	72	73	77	68	82	84	62	62	84	75	7
Pharynx	139	157	143	146	166	132	163	133	133	135	154	132	166	146	13
mbd	155	172	146	152	203	155	163	156	145	139	166	139	203	160	19
abd	93	98	120	98	104	93	87	116	87	87	109	87	120	100	12
Tail length	62	89	90	72	74	87	85	85	78	85	75	72	90	82	7
Amphid length	8	7	9	8	9	10	9	9	9	8	11	7	11	9	1
Amphid aperture	6	7	8	8	8	7	6	7	7	6	8	6	8	7	1
Amphid aperture distance to anterior end	13	15	18	15	16	18	16	17	18	17	19	15	19	17	1
Capsule	49	52	53	53	56	50	52	50	46	47	51	46	56	51	3
Cephalic capsule width posterior edge	42	47	43	46	47	41	46	42	42	42	41	41	47	44	2
Cephalic capsule width anterior edge	21	21	26	26	24	27	26	25	24	22	21	21	27	24	2
Cephalic capsule length	25	31	27	29	29	27	25	27	26	25	25	25	31	27	2
Tropis length	10	9	12	12	12	16	13	12	12	11	10	9	16	12	2
a	32	33	39	34	27	38	33	34	34	30	32	30	29	33	27
b	5	5	5	5	5	6	5	5	5	4	5	4	5	5	9
c	80	63	62	73	74	68	63	61	63	48	71	57	65	64	74

The individuals are indicated by the voucher code. The first individual (2D24C10) is the holotype.
Abbreviations: a, body length/body width; abd, anal body diameter; b, body length/pharynx length; c, body length/tail length; cbd, corresponding body diameter; f, female; m, male; Max., maximum; mbd, maximum body diameter; Min., minimum.

Institute of Natural Science (RBINS) – Brussels, with the accession numbers RIT784 (holotype) and RIT785–RIT787 (paratypes). Three additional paratypes (6D12C10, 3D13C10, and 5D24C10) have been deposited in the Zoology Museum of Ghent University, under the numbers UGMD104120–UGMD104122. DNA material of these seven specimens is available in the Zoology Museum of Ghent University, under the numbers UGMD125007–UGMD125013. DNA sequences of specimen 3D13C10 are available in GenBank under the accession numbers FR853134 (COI), FR853144 (ITS), FR853143 (D2D3).

Description: Body long, cylindrical, and ventrally curved; clearly anteriorly tapered in anterior neck region. Body cuticle smooth except for fine striations in head region and appearing wrinkled (rugose) in posterior precloacal region in male. Eyespot, laterally in anterior neck region conspicuous. Lip region divided into six lips; anterior sensilla arranged in an anterior crown of six inner labial papilla and a second crown of six outer labial and four cephalic setae (2–4 μm long). Cervical setae arranged in six rows. Cephalic capsule well developed, anteriorly with slightly marked lobes and a clear ventral tropis projecting anteriorly. Posterior edge of the cephalic capsule with irregular undulations, more or less attenuated and divided into six lobes by narrow incisions, ending anteriorly in circular fenestrae showing slight variation in shape and leaving space for innervations of anterior sensilla and amphids. In cross-section, two short, pointed subdorsal tropis-like projections in the internal wall of the cephalic capsule visible at level of dorsal tooth. Amphidial fovea shield-shaped to circular, never completely surrounded by the cephalic capsule. Buccal cavity with a short blunt dorsal tooth. Pharynx without bulb, surrounded by nerve ring at about one third of the total pharynx length from anterior end. Cardia with triangular shape, projecting to the lumen of the intestine. Three caudal glands extending anteriorly beyond rectum.

Males: Ventral surface at cloaca level with very minute protuberances until about the most anterior subventral setiform copulatory supplements. The ventromedian copulatory supplement is cyathiform and winged. Pair of curved spicules with the median portion more dilated. Gubernaculum with duplicated apophysis and the crura with membrane embracing the spicule. Gonads diorchic with opposed testes.

Females: Vagina at 62% of the body. Intracuticular granules surrounding the transverse vagina present. Gonads amphidelphic with reflexed ovaries.

Type locality: Specimens collected from stranded holdfasts of *Macrocystis* sp. in Ventura Beach, California, USA.

Remark: The juveniles of both species can be easily confused with juveniles and adults of another common co-occurring nematode species *Thoracostoma microlobatum* (Allgén, 1947). It is because of the fact that the cephalic capsule has several perforations in the juvenile, that tend to fuse or disappear along the development. In *T. microlobatum* those perforations persist until the adulthood. Hence, identifying the species based on juveniles may cause misidentifications.